Supplementary material

S1. GoM-biogeochemical model description and calibration

We used the 20-yr (1993-2012) hydrodynamic model of Zang et al. (2019) to drive the biogeochemical model. The details of model setup, as well as model-observation comparisons of physical variables, were stated in Zang et al. (2019). In this supplementary material we provide additional comparison results of sea surface temperature (SST), nutrients, and chlorophyll to further calibrate the performance of biogeochemical model.

The simulated sea surface temperature (SST) reproduced its seasonal variation and agreed well with observations (Fig. S2). the correlation coefficients of SST at 4 buoy stations (42003, 42007, 42035, and 42036; locations see Fig. S1) were higher than 0.89. For biogeochemical model, we compared concentrations of NO_3, $Si(OH)_4$, and chlorophyll with in-situ observations (World Ocean Database; https://www.nodc.noaa.gov/OC5/WOD/pr_wod.html) and satellite images (MODIS and SeaWiFS). To estimate the model's capacity of reproducing long-term nutrients distributions, we compared multi-year monthly vertical profiles of NO_3 and $Si(OH)_4$ during our simulation period. The model well captured the depletions of NO_3 and $Si(OH)_4$ from the surface layer to 50 m depth, as well as the their gradual increase to the peaks located between 500 and 1000 m depth (Figs. S3 and S4).

Simulated 20-yr seasonal mean surface chlorophyll agreed well with chlorophyll concentration derived from MODIS satellite images (Fig. S5): higher concentration distributed around the Mississippi Delta, suggesting the great contribution of fluvial nutrient supply to intensive photosynthesis and primary production in coastal Louisiana. To further validate temporal variation of chlorophyll, we estimated spatial-averaged monthly mean sea surface chlorophyll concentration over two sub-regions: Mississippi Delta and northern Gulf of Mexico. Among the two sub-regions, Chlorophyll concentration was higher over the Mississippi Delta due to fluvial nutrient discharge (Fig. S6). Seasonal variation of chlorophyll concentration closely matched satellite data, and the correlation coefficients between model results and satellite datasets (MODIS and SeaWiFS) were higher than 0.66.

Fig S1. Model domain and bathymetry. The red polygons indicate locations of two sub-regions. Locations of 4 buoy stations (42035, 42007, 42036 and 42003) are marked as cyan triangles in the map.

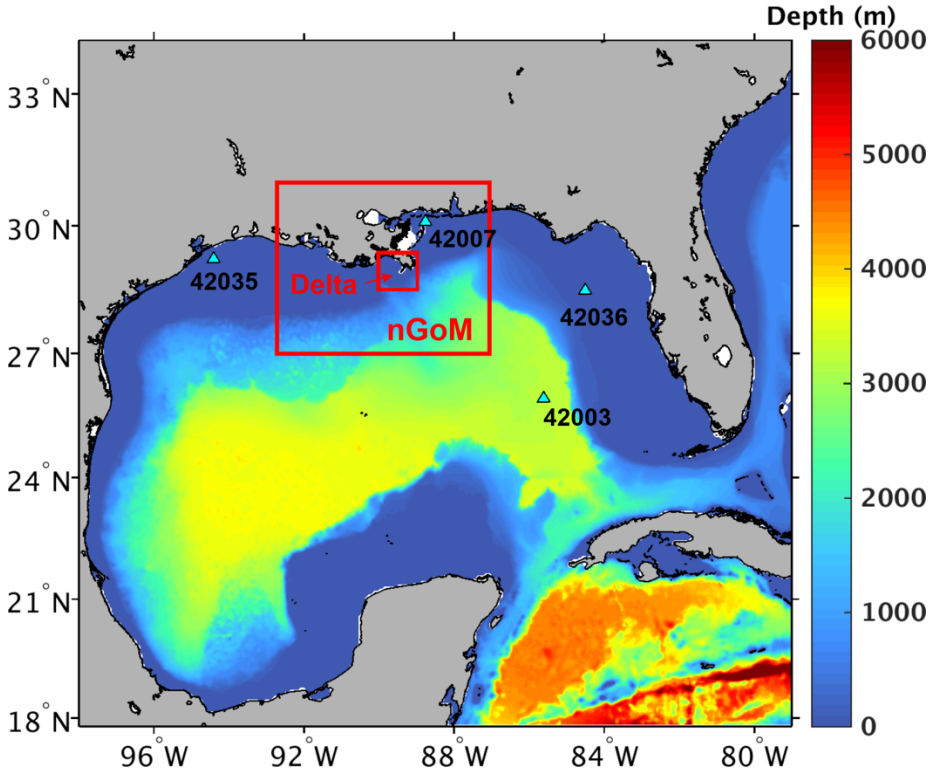

Fig S2. Time series of SST comparison between model results and field measurements at 4 buoy stations (NDBC; https://www.ndbc.noaa.gov).

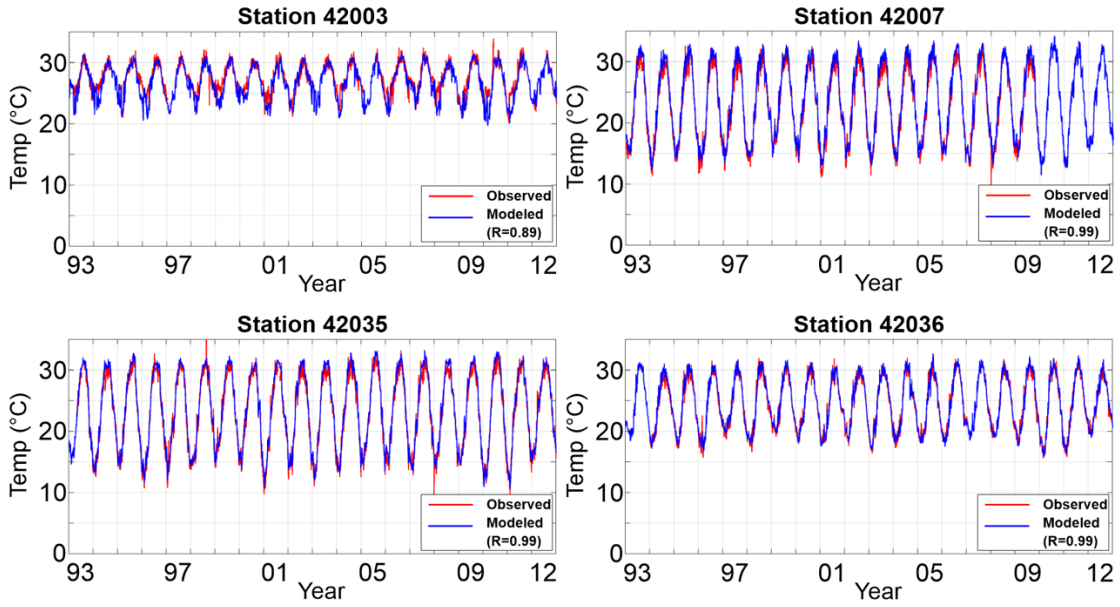

Fig S3. Comparison of multi-year (1993-2012) monthly vertical distributions of NO_3 in the Gulf of Mexico (upper panel) and the locations of field measurements (lower panel); (data source: World Ocean Database; https://www.nodc.noaa.gov/OC5/WOD/pr_wod.html).

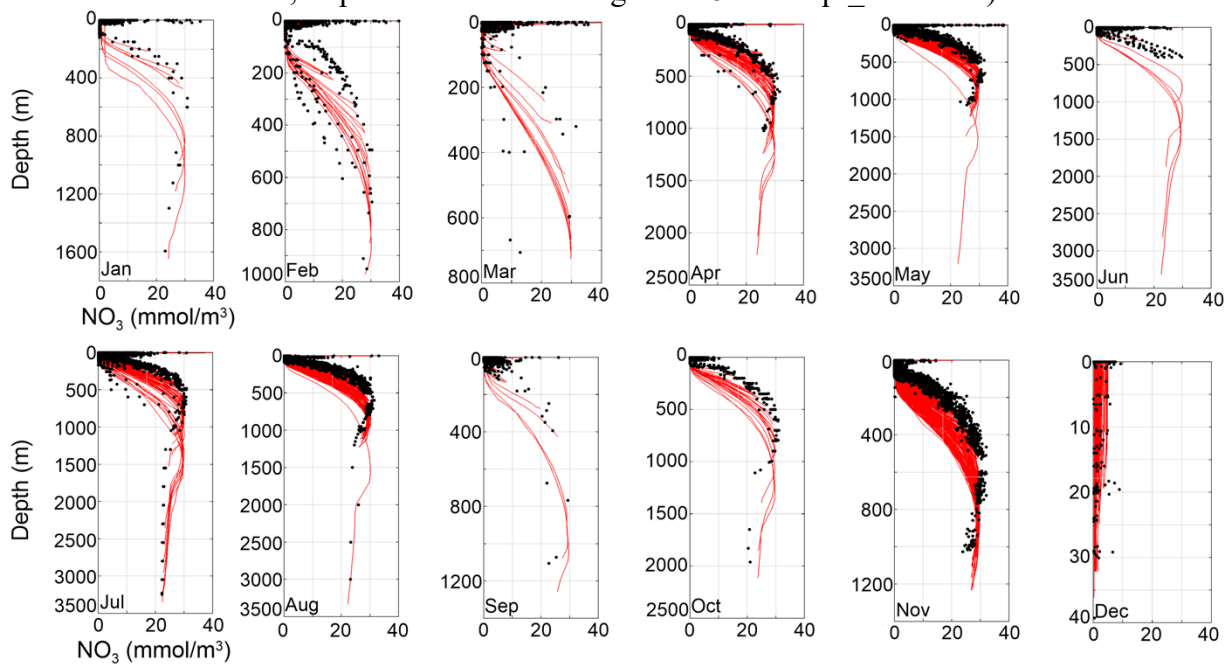

Fig S4. Comparison of multi-year (1993-2012) monthly vertical distributions of $SiOH_4$ in the Gulf of Mexico (upper panel) and the locations of field measurements (lower panel).

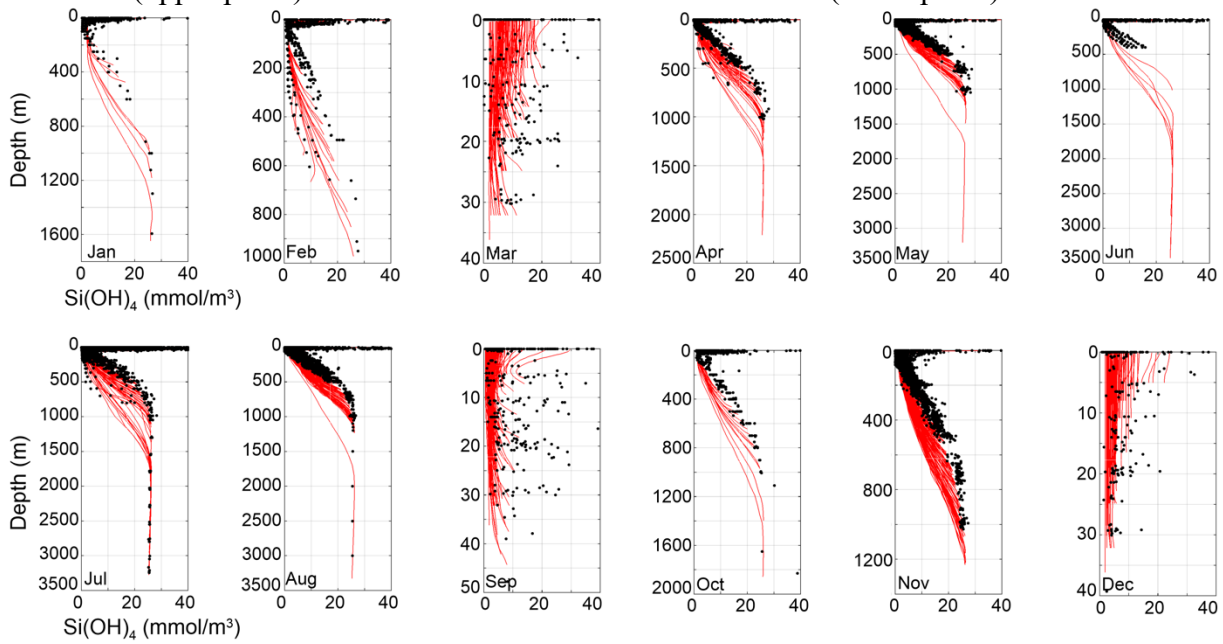

Fig S5. 20-yr seasonal mean sea surface chlorophyll comparison between MODIS (a and b) and model results (c and d) in summer and winter.

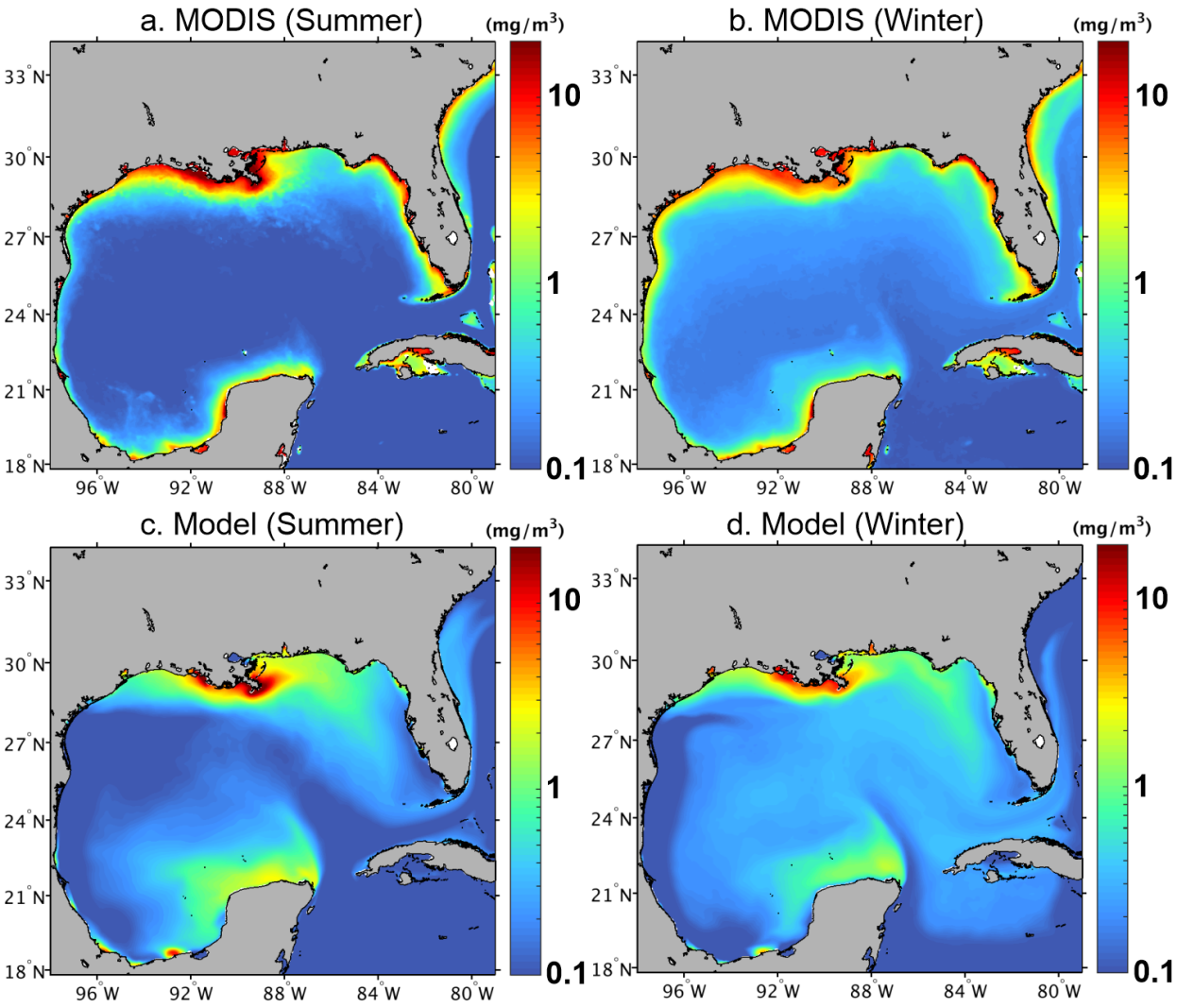

Fig S6. Time series of monthly mean sea surface chlorophyll concentration (unit: mg/m^3) derived from model (black), MODIS (green), and SeaWiFS (red) over the northern Gulf of Mexico (nGoM; panel a) Mississippi Delta (a), and Mississippi Delta (b). Locations of the two sub-regions are shown in Fig. S1.

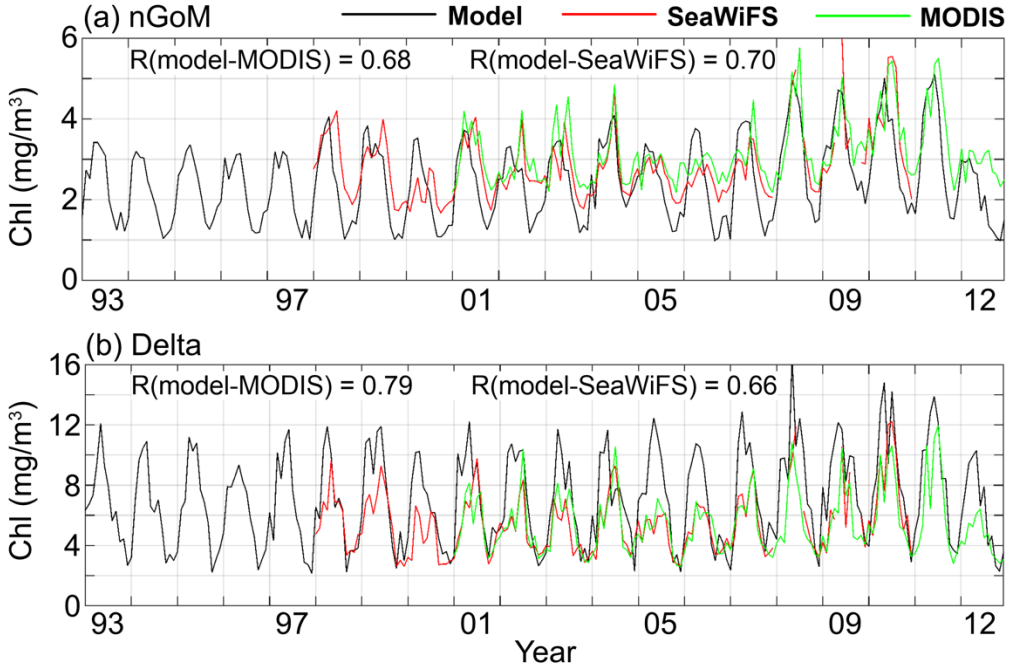

Table S1. NEMURO model parameters (PS: small phytoplankton; PL: large phytoplankton; ZS: small zooplankton; ZL: large zooplankton; ZP: predatory zooplankton)

Parameter	Name				Source
	Phytoplankton parameters	**PS**	**PL**		
PARfrac	Fraction of shortwave radiation for photosynthesis	0.43	0.43		Fennel et al. (2006)
V_{max}	Maximum photosynthetic rate at 0 °C (d^{-1})	0.78	0.56		Gomez et al. (2018)
k_{Gpp}	Temperature coefficient for photosynthesis ($°C^{-1}$)	0.0693	0.0693		Gomez et al. (2018)
α_P	Initial slope of the P-I curve ($m^2\ W^{-1} d^{-1}$)	0.035	0.035		Gomez et al. (2018)
K_{NO3}	Half saturation constant for nitrate (mmol N m^{-3})	1.0	3.0		Kishi et al. (2007)
K_{NH4}	Half saturation constant for ammonium (mmol N m^{-3})	0.5	0.5		Kishi et al. (2007)
K_{Si}	Half saturation constant for Silicate (mmol Si m^{-3})	—	3.0		Kishi et al. (2007)
ϕ_P	Phytoplankton ratio extracellular excretion	0.08	0.08		Kishi et al. (2007)
P_{Mor}	Mortality at 0 °C (m^3 mmol N^{-1} d^{-1})	0.016	0.016		Gomez et al. (2018)
k_{PMor}	Temperature coefficient for mortality ($°C^{-1}$)	0.0588	0.0693		Kishi et al. (2007)
Att_{sw}	Light attenuation due to seawater (m^{-1})	0.04	0.04		Kishi et al. (2007)
Att_p	Light attenuation due to chlorophyll (m^2 $mmol^{-1}$ N)	0.0248	0.0248		Fennel et al. (2006)
	Zooplankton parameters	**ZS**	**ZL**	**ZP**	
GR_{mPS}	Maximum grazing rate at 0 °C on PS (d^{-1})	0.27	0.04	—	Gomez et al. (2017)
GR_{mPL}	Maximum grazing rate at 0 °C on PL (d^{-1})	0.07	0.18	0.3	Gomez et al. (2017)
GR_{mZS}	Maximum grazing rate at 0 °C on ZS (d^{-1})	—	0.14	0.1	Gomez et al. (2017)
GR_{mZL}	Maximum grazing rate at 0 °C on ZL (d^{-1})	—	—	0.1	Gomez et al. (2017)
k_{Gra}	Temperature coefficient for grazing ($°C^{-1}$)	0.053	0.053	0.053	Gomez et al. (2017)
K_{SPZ}	Half saturation constant on PS (mmol N m^{-3})^2	0.17	0.9	—	Gomez et al. (2017)
K_{LPZ}	Half saturation constant on PL (mmol N m^{-3})^2	0.1	0.9	0.2	Gomez et al. (2017)
K_{SZZ}	Half saturation constant on ZS (mmol N m^{-3})^2	—	0.9	0.8	Gomez et al. (2017)
K_{LZZ}	Half saturation constant on ZL (mmol N m^{-3})^2	—	—	0.8	Gomez et al. (2017)
Z_{Mor}	Mortality at 0 °C (m^3 mmol N^{-1} d^{-1})	0.023	0.03	0.0305	Gomez et al. (2018)
k_{ZMor}	Temperature coefficient for mortality ($°C^{-1}$)	0.069	0.069	0.069	Kishi et al. (2007)
α_Z	Assimilation efficiency	0.7	0.7	0.7	Kishi et al. (2007)
β_Z	Growth efficiency	0.3	0.3	0.3	Kishi et al. (2007)
	Particulate matter parameters	**PON**	**Opal**		
ω_P	Sinking rate (m d^{-1})	1.0	10.0		Fennel et al. (2006)
$VP2N_0$	Decomposition rate from PON to NH_4 (d^{-1})	0.1	—		Kishi et al. (2007)
$VP2D_0$	Decomposition rate from PON to DON (d^{-1})	0.1	—		Kishi et al. (2007)
$VO2S_0$	Decomposition rate from Opal to Silicate (d^{-1})	—	0.02		Fennel et al. (2006)
k_{P2N}	Temperature coefficient for decomposition from PON to NH_4 ($°C^{-1}$)	0.0693	—		Kishi et al. (2007)
k_{P2D}	Temperature coefficient for decomposition from PON to DON ($°C^{-1}$)	0.0693	—		Kishi et al. (2007)
k_{O2S}	Temperature coefficient for decomposition from Opal to Silicate ($°C^{-1}$)	—	0.0693		Kishi et al. (2007)